Journal of Materials Science and Engineering A 7 (1-2) (2017) 25-36
doi: 10.17265/2161-6213/2017.1-2.004

Weight-Optimized Bushingless Connecting Rods: Improving the Tribological Performance of a Gudgeon Pin/Connecting Rod System by Using the Triboconditioning® Process

Jonas Lundmark[1], Boris Zhmud[1], Boris Brodmann[2], Dietmar Schorr[3] and Urban Morawitz[4]

1. Applied Nano Surfaces Sweden AB, Uppsala SE-75323, Sweden

2. OptoSurf GmbH, Ettlingen D-76275, Germany

3. Steinbeis Transfer Center Tribology, Karlsruhe D-76133, Germany

4. Ford Motor Company, Cologne D-50735, Germany

Abstract: The risk of failures associated with a distressed pin/connecting rod bearing contact without forced pin oiling is exaggerated due to ever increasing power density and torque output of modern TSI (turbocharged straight injection) and TDI (turbocharged direct injection) engines, in combination with the introduction of low-viscosity low-SAPS (sulfated ash, phosphorus, sulfur) lubricants and general engine downsizing resulting in fewer cylinders to bear the load. This forces OEMs (original equipment manufacturer) to look for innovative cost-efficient solutions to promote bushingless connecting rods without impacting reliability. One such solution is the Triboconditioning® process. Triboconditioning is an industrial surface finishing process which attempts to carry out running-in of components during their manufacture. The present paper provides an in-depth analysis of the tribological effects of Triboconditioning® on the pin/conrod contact.

Key words: Triboconditioning, mechanochemical finishing, connecting rod, wear, tribology.

1. Introduction

The connecting rod connects the piston to the crankshaft, transforming the axial motion of the piston into the rotation of the crankshaft. The connecting rod consists of the crank or big end, pin or small end, and shank. In a working engine, the connecting rods are subjected to a number of stresses: compression due to gas pressure in the power cycle after the TDC (top dead center) firing, alternating compression and tension due to inertia forces in the reversal points, and bending due to its pivoting movements. In order to improve engine efficiency and to minimize vibrations, it is desirable to reduce reciprocating masses (piston and connecting rod) to a minimum. For instance, in motor sports, H-shaped shanks are preferred for this particular reason. Use of a bushingless pin bearing in the small end is another way to reduce oscillating masses, which is of increasing importance in modern passenger car engines due to stringent fuel economy requirements [1, 2].

The majority of connecting rods are manufactured from precipitation-hardening ferritic-pearlitic steels, and aka AFP steels. The current industry standard for fracture splitting steel grades is C70S6, an air cooled pearlitic steel containing 0.7% C. Newer materials include high strength micro alloyed medium carbon steels, such as 36MnVS4 and 70MnVS4 [1].

One disadvantage of bushingless pin bearing is its inferior cooling, especially if there is no forced pin oiling. This can be partly attributed to poorer heat conductivity and poorer oil affinity of DLC-coatings

Corresponding author: Boris Zhmud, Ph.D., assoc. prof., research fields: applied surface chemistry, mechanochemical processes, tribology and lubrication engineering.

(diamond like carbon) which are almost universally used for the pin protection in the bushingless design. Excessive heat generation due to starved lubrication leads to further oil film thinning, and eventually to a damage of DLC-coating, followed by rapid wear of pin and pin bearing. In some cases, pin boss also gets worn out and eventually pin may work loose. Unfortunately, at the moment, there is no universal standard—something analogous to ASTM (the American Society for Testing and Materials) D 5966 used for evaluating roller follower pin wear—regulating piston pin wear. Hence, judgement of what is an acceptable wear level and what is not is rather subjective and is usually based on failure modes and effects analysis: the risk of failures associated with a distressed pin/connecting rod bearing contact without forced pin oiling is exaggerated due to ever increasing power density and torque output of modern TSI (turbocharged straight injection) and TDI (turbocharged direct injection) engines, in combination with the introduction of low-viscosity low-SAPS (sulfated ash, phosphorus, sulfur) lubricants and general engine downsizing resulting in fewer cylinders to bear the load. In modern engines, the maximum stress at the small end may be in excess of 100 MPa. This forces OEMs (original equipment manufacturer) to look for innovative cost-efficient solutions to promote bushingless connecting rods without impacting reliability. One such solution is the Triboconditioning® process. Triboconditioning is an industrial surface finishing process which attempts to carry out running-in of components during their manufacture. By applying the Triboconditioning® treatment on the bearing surface of the small connecting rod eye, the tribological performance of the pin/conrod tribocouple can be significantly improved leading the way to cost savings and component light weighting [3, 4].

2. Experimental

2.1 Triboconditioning

Connecting rods from a stock TSI gasoline i4 engine was chosen for this study. The bushing less bearing surface of the small eye was triboconditioned using a 4-slot Diahon coolEX honing tool equipped with cemented tungsten carbide ledges (see Fig. 1). Basic process and tooling design are described elsewhere [5, 6]. The process fluid is pumped into the tool through the spindle creating the expansion of the ledges and pressing them against the small eye surface. The tool spins and simultaneously oscillates in the axial direction to provide a uniform surface finish. The tool and the work piece are continuously flushed with the process fluid which feeds reagents for the chemical reaction, and at the same time, provides lubrication and cooling.

2.2 Surface Analysis

2.2.1 Angle Resolved Light Scattering

Angle-resolved light scattering measurements including the determination of variance of angular distribution of scattered light (Aq-value) were carried out using OptoSurf equipment from OptoSurf GmbH.

Table 1 Connecting rod/pin material combinations in study.

Wrist pin	Connecting rod
Steel	Steel + Triboconditioning
Steel	Steel + Mn phosphate
Steel + DLC	Steel
Steel + DLC	Steel + bronze bushing
Steel	Steel + burnishing

Fig. 1 Triboconditioning tool used for the treatment of small eye bearing surface.

2.2.2 Photothermal Analysis

The photothermal analysis is a non-destructive surface-sensitive method which uses a simple physical principle: a diode laser beam creates a hot spot at the surface of a sample in study. The resulting thermal expansion of the material generates an acoustic wave in the sample. The effective penetration depth depends on laser modulation frequency and material properties; the characteristic range for steel is from 10 to 2,000 um, see Fig. 2. Reflected IR radiation is then focused by a thermal lens onto an IR detector. The signal from the latter is digitally processed and the difference in amplitude and phase between modulated laser and detected radiation is determined. The phase shift and amplitude damping depend on the thermal conductivity and specific heat capacity of the sample material. Thus, any differences in the structural density of the material—including those originating from impurities, dislocations, cracks, or density fluctuations due to compression or stretching—can be detected [7, 8].

2.2.3 Stylus Profilometry

Surface roughness of triboconditioned bearing surfaces was characterized according to ISO 4287 using the stylus method (M1 perthometer from Mahr).

2.2.4 Wear Quantification

Wear volume loss for the small eye bearing surface was quantified after the friction test completion by using a 3D coordinate measuring machine Zeiss Prismo. Deviation measured over three coaxial tracks, one in the middle, and two by sides, was used as a basis for the wear depth determination.

2.2.5 Surface Integrity and Wear Pattern

Surface integrity and wear patterns were examined with Keyence Color 3D Laser Scanning Microscope VK-9700.

3. Results and Discussion

In general, the Triboconditioning treatment results in the development of a progressively plateaued roughness profile with reduced R_a, R_{pk}, and increasingly negative skewness with a reduced S_{pk}/S_{vk} ratio [9]. This fact is evidenced by angle-resolved light scattering measurements, which show a drop in the variance of angular distribution of scattered light (A_q-value) for triboconditioned surfaces. See Fig. 3.

To explain why this happens, let’s take a look at Fig. 4 in which three simulated one-dimensional roughness profiles are presented. The profiles were assigned progressively negative skewness and decreasing R_a, R_{pk}, and R_k values in order to mimic the topographical changes caused by Triboconditioning, cf. Fig. 5. Then, for each profile, scattered light intensity distribution function, $I(\varphi)$, and the corresponding variance of angular distribution of scattered light (A_q-value) are calculated. In this case, a lower A_q value indicates lower surface roughness, since a smoother surface reflects a narrower beam [9].

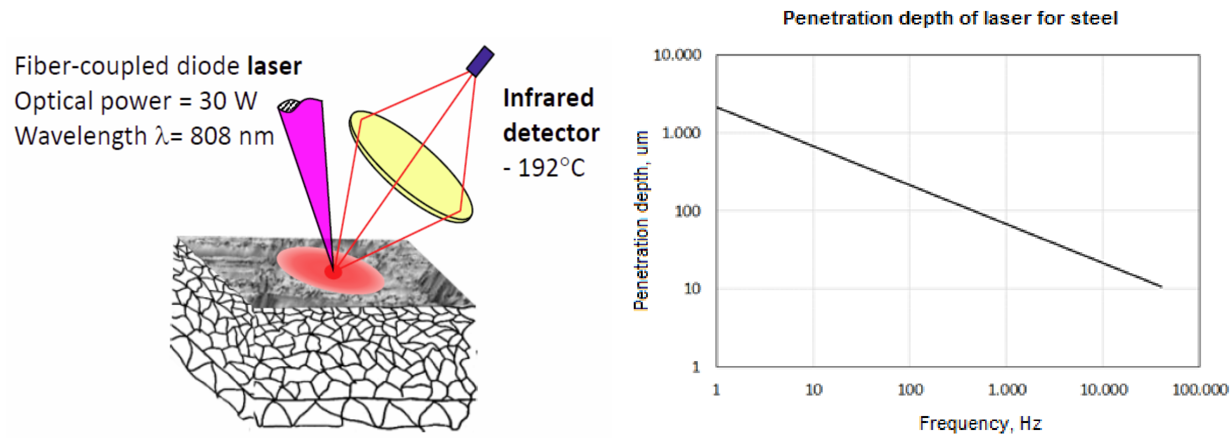

Fig. 2 The underlying physical principle of photothermal analysis.

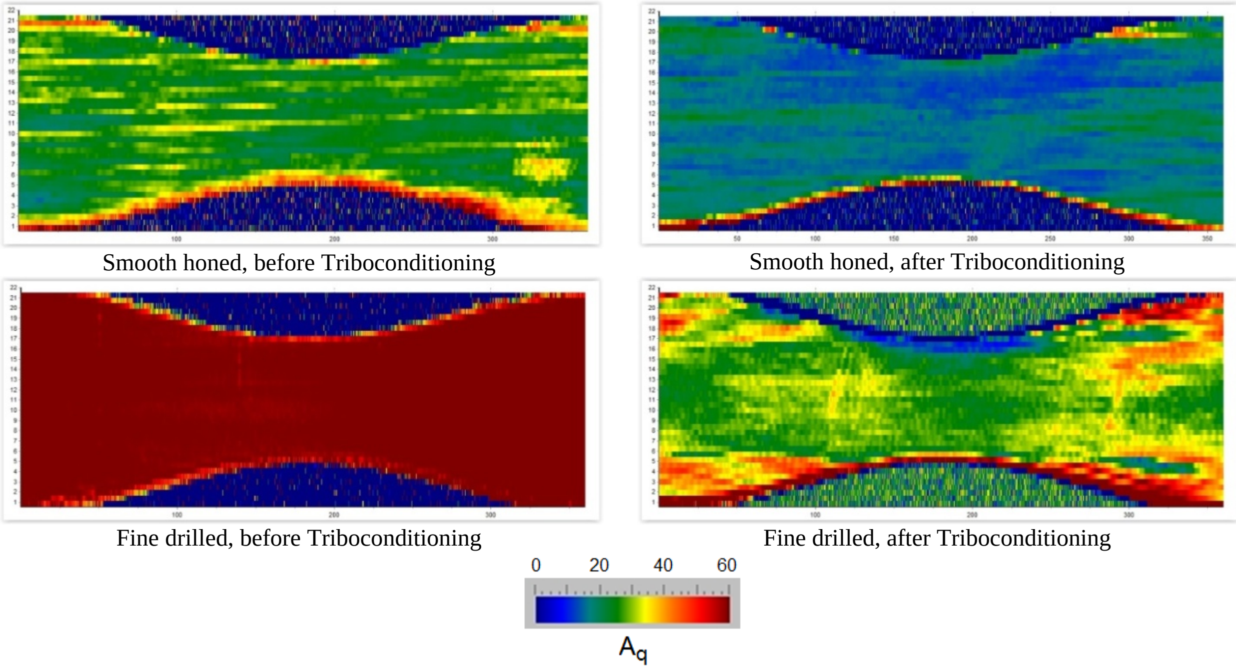

Fig. 3 Surface mapping of the variance of angular distribution of scattered light (A_q-value) for the small eye bearing surface. A decrease in the A_q value reflects plateauing the surface roughness profile due to the Triboconditioning treatment.

In previous studies, it has been found that Triboconditioning treatment leads to the formation of a thin non-stoichiometric tribolayer, which is ca 100 nm thick [10, 11]. At the same time, it generates compressive stresses in the underlying subsurface. The depth of the compressive stress zone is material dependent. Assuming that peak contact stresses for asperity-asperity contacts occurring between the triboconditioning tool and the workpiece have the same order of magnitude as the workpiece material yield stress, it is possible to predict that the compressive stress zone may stretch from a few tens up to a hundred micrometers in depth for steel and cast iron components. This agrees with the results of residual stress measurements on shot-peened and roller-burnished surfaces [12].

Photothermal measurements provide indirect indication of the “deformation zone” depth of ca 10 um (see Fig. 6).

The triboconditioned small end bearings of the connecting rods in study were dissected into halves and the material properties were investigated using the photothermal method. Two types of measurements were carried out:

(i) Measuring the properties at two different points, P1 and P2, the probing depth ranges from 18 to 11 µm; see Fig. 7a.

(ii) Measuring the properties with a probing depth of 12.5 µm over an area of 9 mm × 120^o, see Fig. 7b.

The corresponding phase shift data are presented in Figs. 8a, 8b, and 9. As can be seen, measurable differences in phase shift between the triboconditioned parts and untreated references, for both fine drilled and smooth honed variants. The differences are more pronounced for smooth honed surfaces.

Figs. 10a-10e show the surface condition of different bearing surfaces before and after the tribotest. As can be seen, Triboconditioned small eye bearing surface shows very little wear when tested against a steel pin. In terms of tribological performance, the combination steel pin/triboconditioned small eye turns out be as good as DLC-coated pin/honed small eye, and outperforms all other combinations. This concerns both friction (Fig. 11) and wear (Fig. 12). It is interesting that both bronze bushing and phosphated small eye bearings show abnormally high abrasive wear

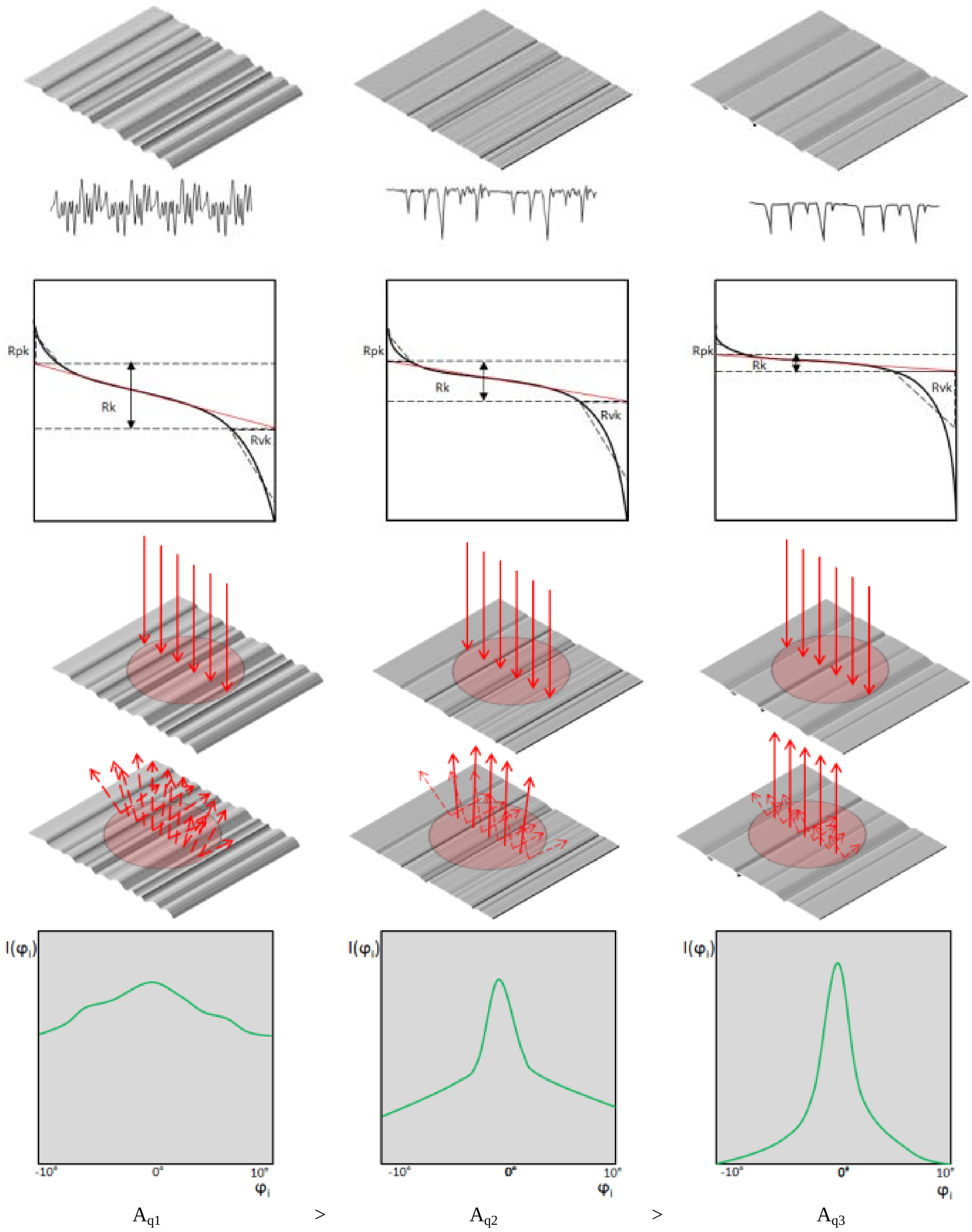

Fig. 4 Simulated light scattering. Decrease in surface roughness results in lower A_q values.

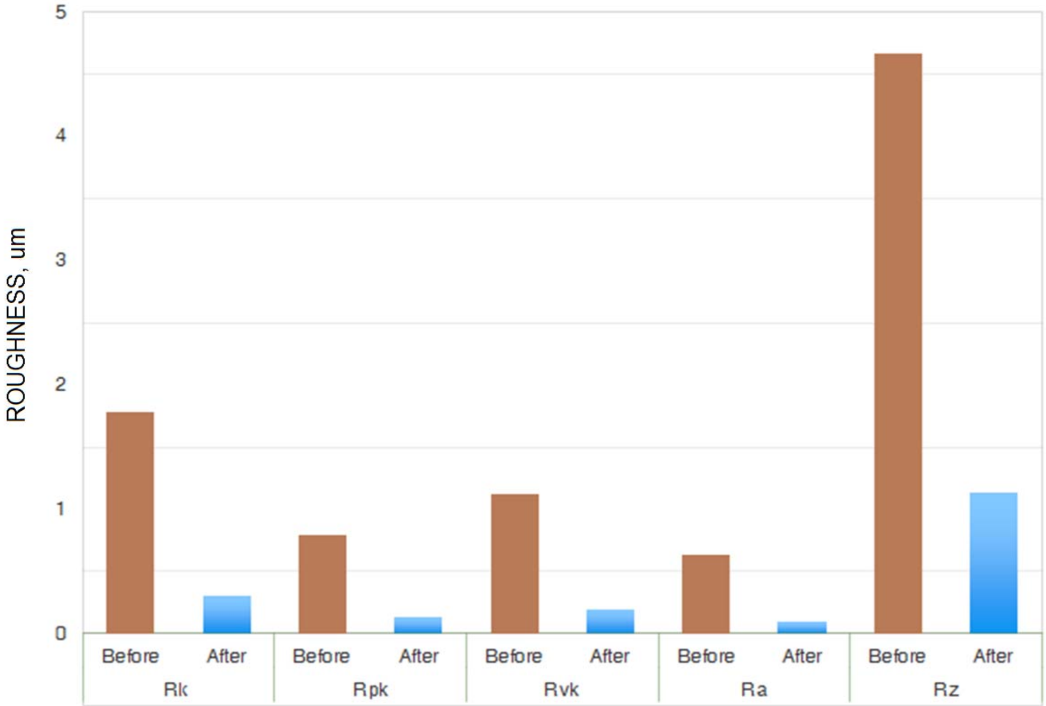

Fig. 5 Change in the surface roughness of the small eye bearing surface due to Triboconditioning.

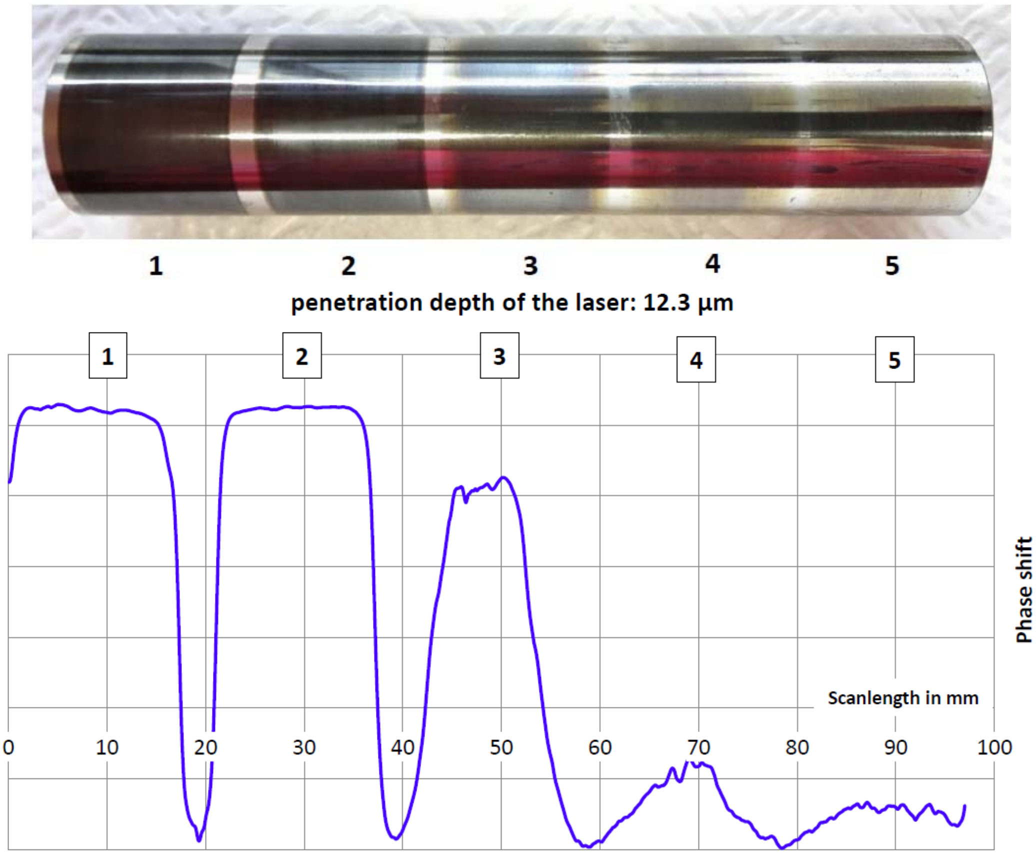

Fig. 6 Phase shift measured with the photothermal technique for a reference shaft with five different zones triboconditioned under progressively declining loads from 5 to 1 kN. Significant differences between the sections due to microstructure changes in the material are detected at a depth of 11-14 µm.

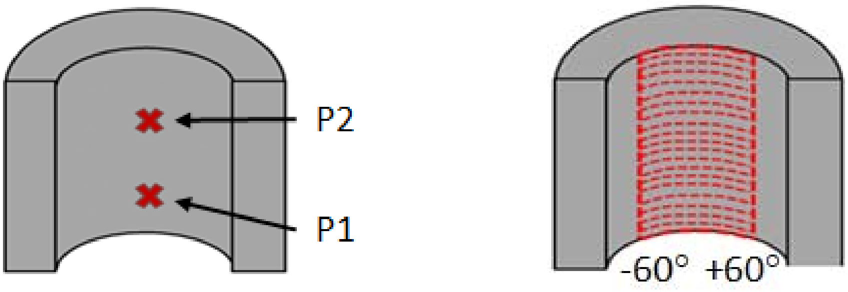

(a) (b)

Fig. 7 Analysis zones for photothermal investigation of the material properties at the small eye bearing surface.

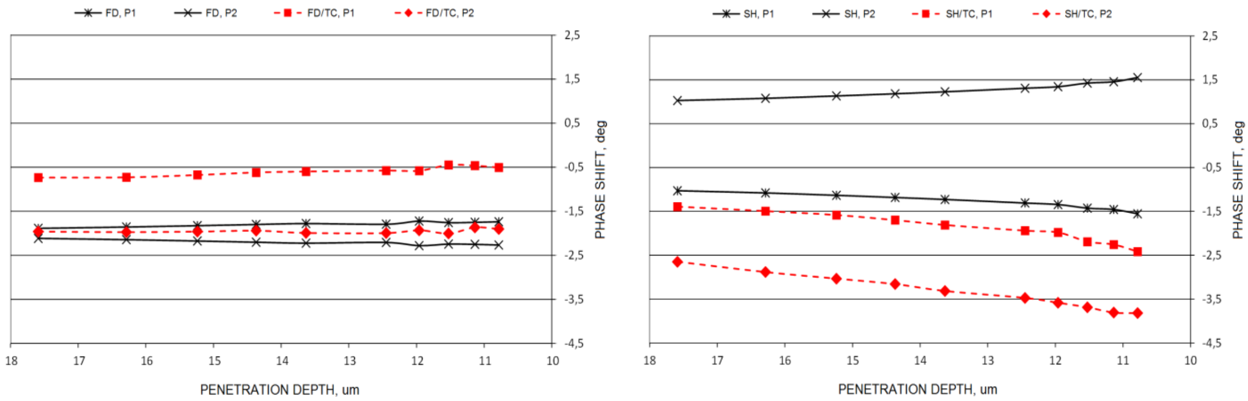

(a) (b)

Fig. 8 Results of the photothermal depth scanning: the phase shifts for the Triboconditioned bearing surfaces, FD/TC and SH/TC, reflect microstructure changes in the subsurface material penetrating down to 11-18 μm depth; (a) the reference surface was FD (fine-drilled); (b) the reference surface was SH (smooth honed).

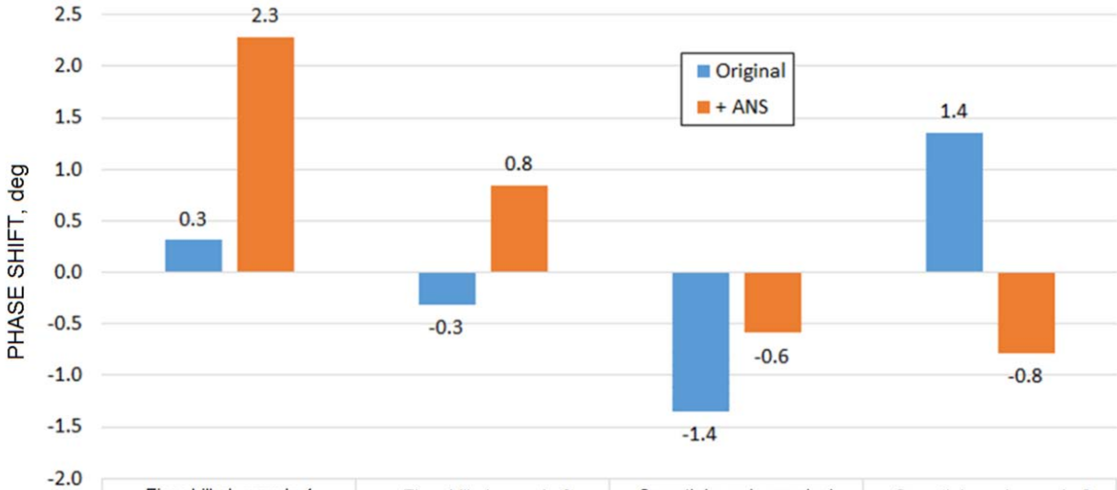

	Fine drilled, sample 1	Fine drilled, sample 2	Smooth honed, sample 1	Smooth honed, sample 2
Original	0.3	-0.3	-1.4	1.4
+ ANS	2.3	0.8	-0.6	-0.8

Fig. 9 Average phase shifts detected by the photothermal method at 12.5 μm probing depth.

SURFACE CONDITION: TRIBOCONDITIONED CONROD

Before test

After test against steel pin

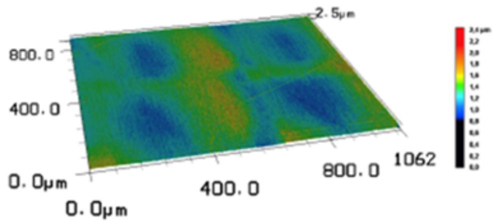

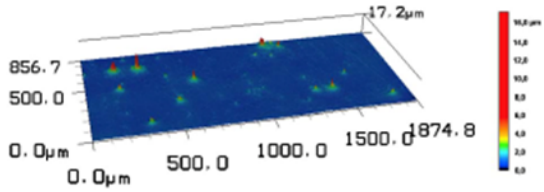

um	Before	After
R_a	0.18	0.20
R_{pk}	0.24	0.60
R_k	0.46	0.40
R_{vk}	0.12	0.14

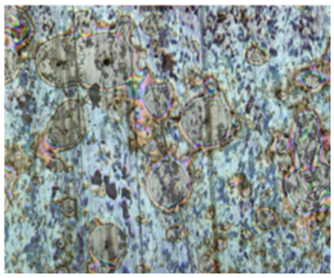

(a)

SURFACE CONDITION: STEEL CONROD

Steel conrod before test

Steel conrod after test with DLC pin

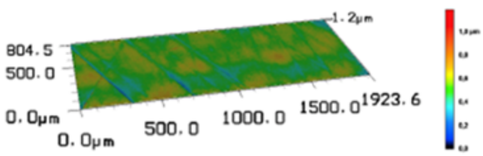

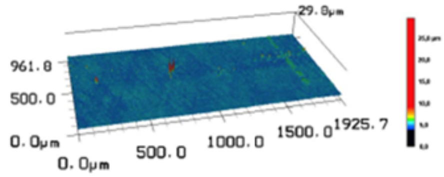

um	Before	After
R_a	0.05	0.27
R_{pk}	0.06	0.62
R_k	0.15	0.62
R_{vk}	0.09	0.15

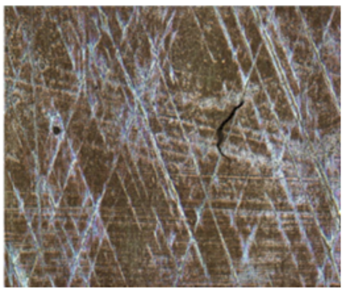

(b)

SURFACE CONDITION: BRONZE BUSHING

Before test

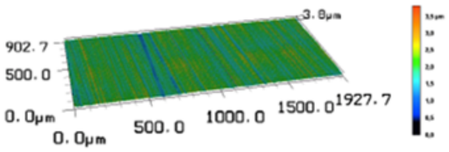

After test with DLC pin

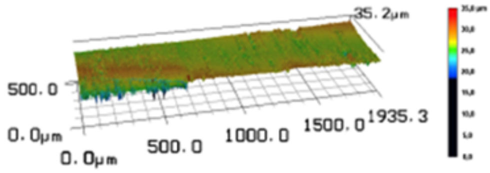

um	Before	After
R_a	0.26	0.57
R_{pk}	0.39	0.80
R_k	0.76	1.21
R_{vk}	0.32	1.65

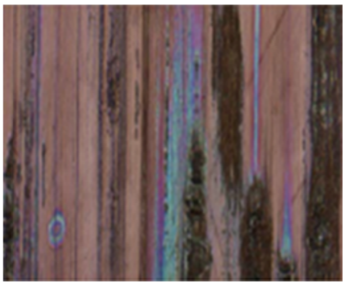

(c)

SURFACE CONDITION: PHOSPHATED

Before test

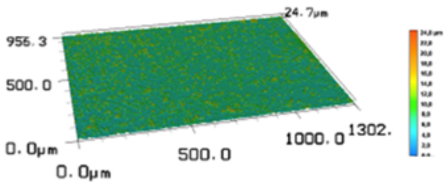

After test with steel pin

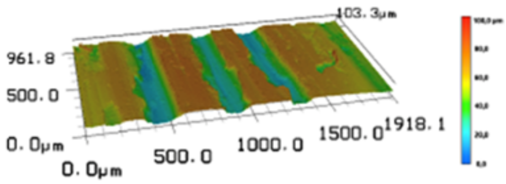

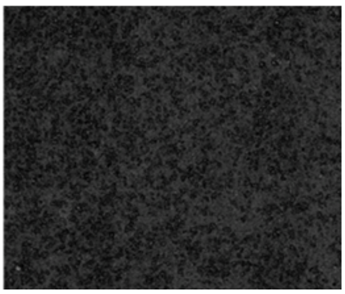

um	Before	After
R_a	1.97	12.2
R_{pk}	4.38	12.6
R_k	4.24	25.8
R_{vk}	1.47	22.5

(d)

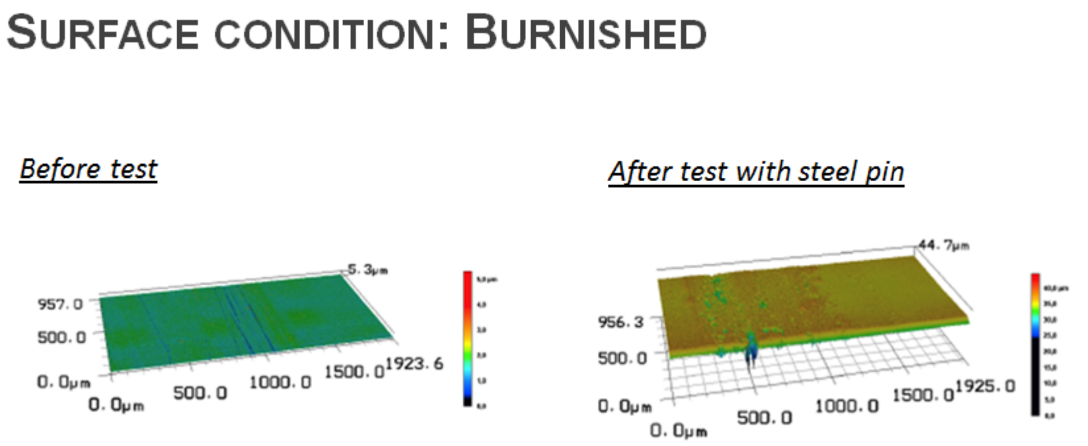

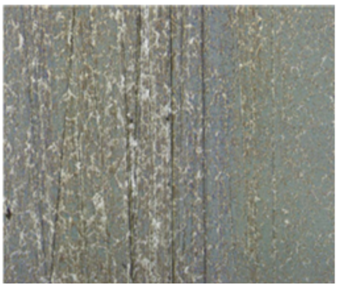

um	Before	After
R_a	0.12	0.47
R_{pk}	0.20	0.56
R_k	0.33	0.76
R_{vk}	0.17	2.49

(e)

Fig. 10 (a-e): Surface condition of the small eye bearing surface before and after the tribotest.

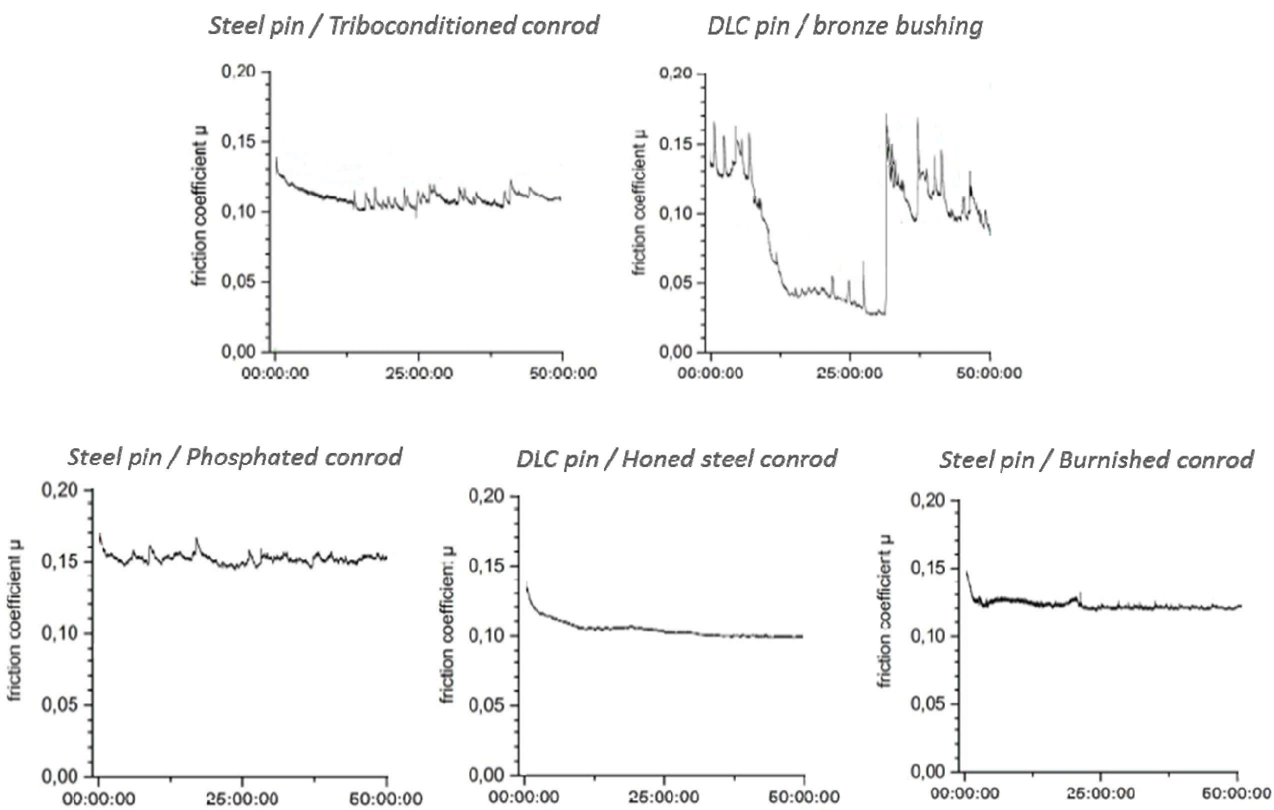

Fig. 11 The coefficient of friction between the pin and the connecting rod for different material combinations.

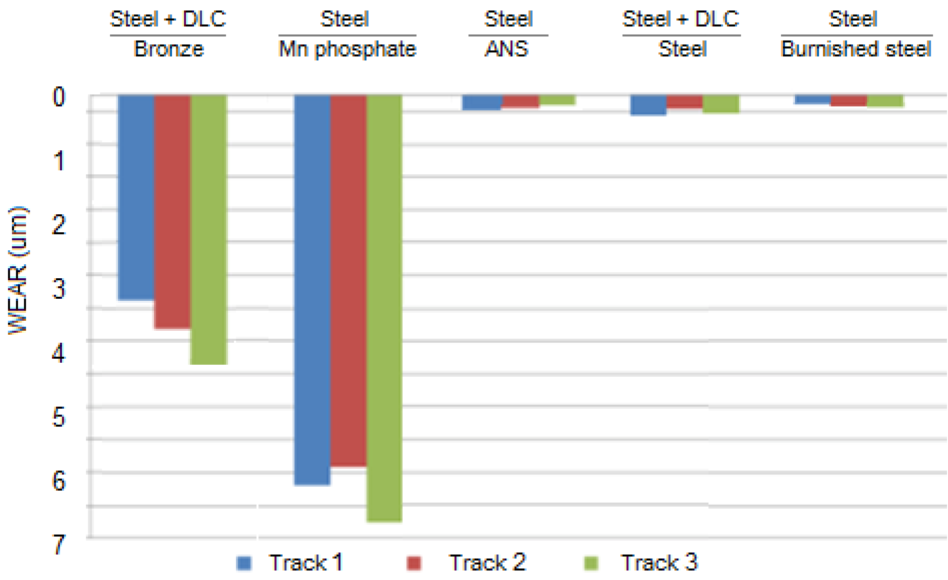

Fig. 12 Average wear depth at the small eye bearing surface after the tribotest.

levels under the tribotest conditions. This should be taken as a warning sign: these materials are more likely to fail in boosted engines unless the load-bearing surface is properly scaled up, herewith use of lower viscosity crankcase lubricants of ACEA C1, C2, A5/B5, and the forthcoming ACEA C5, API FA-4 and ILSAC GF-6b specifications are associated with a higher failure risk. It should be noted that burnished bearing surface, while showing relatively small wear, has developed micro pitting damage and thus also failed the assessment criteria.

4. Conclusion

These presented results suggest conclusively that the Triboconditioning® treatment on the bearing surface of the small eye bearing surface of connecting rods is beneficial for the tribological performance of the pin/conrod tribosystem.

Acknowledgements

We appreciate the help with production trials and testing from the following people: Dipl. Ing. Udo Schleif, Dipl. Ing. André Schmiedel, Dipl. Ing. Frank Pfab from Linamar, and Dipl. Ing. Udo Eckert, and Dipl. Ing. Torsten Schmidt from Fraunhofer IWM.

References

[1] Hart, K., Azevedo, M., Rebello, J., and Ribeiro, C. 2003. “Bushingless Piston and Connecting Rod Assembly and Method of Manufacture.” US 6557457, Federal Mogul.

[2] Mahle, G. S. (ed.) 2010. *Cylinder Components: Properties, Applications, Materials.*

[3] Zhmud, B. 2016. “In-manufacture Running-in of Engine Components by Using the Triboconditioning Process: Compatibility with PC-11 and ILSAC GF-6 Motor Oils.” In *Proc. 71st STLE Annual Meeting*, Las Vegas, USA.

[4] Zhmud, B., and Lundmark, J. 2016. “Improving the Tribological Performance of a Gudgeon Pin/Connecting Rod System by Using the Triboconditioning® Process.” In *Proceedings of VDI-conference Zylinderlaufbahn, Kolben, Pleuel*, Baden-Baden, Germany.

[5] Zhmud, B. 2013. “Method for Providing a Low-friction Surface.” US 20130104357, Applied Nano Surfaces Sweden AB.

[6] Granlund, M., Lundmark, J., and Zhmud, B. 2016. “Mechanochemical Conditioning Tool.” WO 2016089289, Applied Nano Surfaces Sweden AB.

[7] Bialkowski, S. E. 1996. “Photothermal Spectroscopy Methods for Chemical Analysis.” Vol. 134. In *Chemical Analysis: A Series of Monographs on Analytical Chemistry and Its Applications*, edited by Winefordner, J. D. Wiley, 584, ISBN 0-471-57467-8.

[8] Schorr, D. 2015. “Photothermie to Characterize Tribological Properties.” In *Anton Paar TriTec SA Users’ Meeting 2015-Advanced Mechanical Surface Testing*, Graz, Austria.

[9] Berg, M., Brodmann, B., Lemel, F., and Zhmud, B. 2016.

"Use of Angle-Resolved Light Scattering, X-ray Fluorescence Spectroscopy and Eddy Current Conductivity Measurements for Surface Condition Monitoring in a Mechanochemical Surface Finishing Process." In *Proc. 20th International Colloquium Tribology-Industrial and Automotive Lubrication*, Stuttgart/Ostfildern, Germany.

[10] Zhmud, B., Tomanik, E., and Xavier, F. A. 2014. "Tribology, Surface Chemistry and Morphology of WS2 Tribofilms Generated by the ANS Triboconditioning Process." *Lubrication Science* 26: 277.

[11] Zhmud, B., and Berg, M. 2014. "Tribology, Surface Chemistry and Morphology of Tribofilms Generated by Mechanochemical Surface Finishing." In *Proc. 19th International Colloquium Tribology-industrial and Automotive Lubrication*, Stuttgart, Germany.

[12] Prevéy, P. S. 1981. "The Uniformity of Shot Peening Induced Stress." In *Proceedings of Residual Stress for Designers & Metallurgists, American Society for Metals, Metals Park*, 151-68.